Multiphonon electron capture on mercury vacancy states in „wide-bandgap“ layers of HgCdTe

© N.A. Bekin, D.V. Kozlov

Institute of Physics of Microstructures, Russian Academy of Sciences,
603950 Nizhny Novgorod, Russia

E-mail: nbekin@ipmras.ru

Received October 27, 2025
Revised November 12, 2025
Accepted November 12, 2025

Using the adiabatic approximation, the capture coefficient of conduction band electrons on A_2^{-2} mercury vacancy levels in HgCdTe semiconductors with a band gap of more than ~ 100 meV (with a Cd fraction in the solution $x > 0.2$) was estimated. It is shown that electron capture on the vacancies is significantly suppressed with an increase in the cadmium content. For example, the low-temperature capture coefficient decreases from $\sim 10^{-8}$ cm$^3 \cdot$ s^{-1} at $x = 0.21$ to $\sim 10^{-12}$ cm$^3 \cdot$ s^{-1} at $x = 0.25$. The low rate of electron capture in wide-bandgap HgCdTe layers is mainly due to the significant distance of mercury vacancy levels from the bottom of the conduction band, as well as the moderately weak electron-phonon coupling of electrons localized in vacancies (Huang-Rhys factor $S < 0.5$).

Keywords: deep defects, mercury vacancies, HgCdTe, multiphonon electron capture, adiabatic approximation.

DOI: 10.61011/SC.2025.08.62599.8701

1. Introduction

Ternary compound of mercury, cadmium and telluride (MCT) is attractive from the point of view of applications and studying of a number of specific fundamental effects [1–4], applications in infrared detection [5] and laser generation [6,7]. Depending on the cadmium content in the $Hg_{1-x}Cd_xTe$ solution, its band gap varies from zero to 1.6 eV in CdTe (at low temperatures). An important characteristic of MCT semiconductors for their applications in optoelectronics is the lifetime of charge carriers in bands with respect to nonradiative transitions to defect levels in the band gap or during interband recombination. Electron capture on defects is interesting both in itself and as a stage in the Shockley-Read-Hall (SRH) recombination process [8,9]. This paper theoretically analyzes the electron capture on mercury vacancies, i.e. defects that almost inevitably appear in MCT solutions due to the weak Hg−Te bond.

Mercury vacancies are double acceptors that can have three charge states: A_2^{-2}-center (no holes are bound to the acceptor), A_2^{-1}-center (one hole is bound), and A_2^0-center (two holes are bound). In the narrow-bandgap layers of the MCT, the capture of electrons and holes on vacancies was studied for the case when it occurs during the emission of single optical phonons [10]. In wider-bandgap materials, this process was considered in a quasi-classical version of the adiabatic approximation [11], which is valid for sufficiently high temperatures. It is shown that for „narrow-bandgap“ MCT layers ($x < 0.2$), interband nonradiative recombination through mercury vacancies can dominate Auger processes at moderate electron concentrations. In this paper, we study electron capture on vacancies in „wide-bandgap“ MCT layers ($x > 0.2$) and use the Born-Oppenheimer quantum approach [12], which is applicable for arbitrary temperatures. We limited ourselves to considering the capture at A_2^{-1}-centers, whose levels are more close to the conduction band [13], and therefore the capture of conduction band electrons on them is expected to be faster.

The calculations used model two-component wave functions, the parameters of which were selected taking into account the solution of the Schrodinger equation with the Kane Hamiltonian 6×6 with the inclusion of the conduction band, heavy and light hole bands. One of the components of the model function corresponds to the conduction band, the second to the valence band, and its parameters characterize the contribution of the conduction band and the valence band to the Kane wave function and take into account the difference in the localization scales of the components corresponding to these bands. The vibronic effects caused by the degeneracy of the vacancy level [14] were ignored, and thus the dynamics of the electron-vibrational motion was described by the factorized wave function of the adiabatic approximation, as for singlet levels. Since the localization radius of the electron wave function on the vacancy is more than 2 times higher than the lattice constant of the solution, we took into account the interaction of electrons only with bulk phonon modes. Only optical phonons were included in the consideration, and the model of dispersion-free phonons was used [15].

Vacancy levels are largely tied to the top of the valence band and, thus, are removed from the bottom of the conduction band in wide-bandgap layers. In addition, the contribution of the conduction band to the vacancy wave function decreases exponentially with an increase in the proportion of cadmium in the MCT layers. These two circumstances are the main reasons for the sharp decrease

in the rate of electron capture on mercury vacancies with an increase in the cadmium content in the solution. The article discusses quantitative discrepancies with the results of semi-classical calculations [11], which are caused by the authors' use [11] of approximations outside the temperature range of their applicability. Nevertheless, this study confirms and even reinforces the conclusion that defects deeper than mercury vacancies should play a significant role in nonradiative SRH recombination in wide-bandgap MCT layers.

2. Calculation method

2.1. Energy and wave functions of the adiabatic approximation

An electron bound on a defect and interacting with lattice vibrations can be described by an adiabatic approximation wave function $\Psi(\mathbf{r}, \eta) = \psi(\mathbf{r}, \eta)\chi(\eta)$, which obeys the Born-Oppenheimer equation system [12], where $\psi(\mathbf{r}, \eta)$ and $\chi(\eta)$ are the wave functions of the electron and phonons, respectively; $\mathbf{r}$ is the radius vector of the electron, η is the set of normal coordinates of the oscillatory motion of the crystal.

For moderately deep defects, the energy of the electron-phonon interaction is well approximated by the expression linear in normal coordinates η (or the phonon creation and destruction operators):

$$H_{eL} = \Sigma_{\sigma,\lambda,\mathbf{q}} u_{\sigma\lambda\mathbf{q}}(\mathbf{r})\eta_{\sigma\lambda\mathbf{q}}, \tag{1}$$

where σ numbers the branches of the law of dispersion, λ is the type of standing wave of crystal vibrations (cos-type or sin-type), $\mathbf{q}$ is the phonon wave vector; $\eta_{\sigma\lambda\mathbf{q}}$ are real normal coordinates measured in units $[\hbar/(M\omega_{\sigma\mathbf{q}})]^{1/2}$, $\omega_{\sigma\mathbf{q}}$ is the phonon frequency, M is the mass of the lattice oscillator. Summation by $\mathbf{q}$ is carried out here and further for half of the Brillouin zone. Estimates are given in Ref. [16] for four types of electron-phonon interaction in polar semiconductors, i. e., for deformation-acoustic (DA), deformation-optical (DO), piezoacoustic (PA) and polar optical (PO) interactions. It is shown that, the intensity of these four types of interactions (DA, DO, PA, and PO) in the order of magnitude are related as $(qa_0)^2 : qa_0 : qa_0 : 1$, where q is the modulus of the phonon wave vector, and a_0 is the lattice constant. Since qa_0 is a small parameter for wave vectors with a modulus smaller than the size of the Brillouin zone, it can be assumed that the electrostatic macrofield is the dominant mechanism of electron-phonon interaction in polar semiconductors [16] (Fröhlich interaction). We extrapolate the expressions for the interaction energy to the entire Brillouin zone, including short-wavelength phonons, for which the macrofield approximation is not strictly applicable. However, given the relatively large scale of localization of the vacancy wave function, this is a good approximation. In addition, we will take into account the interaction only with LO-phonons, and we will further omit the index σ, numbering the branches of the dispersion law.

Based on the expressions from Ref. [16] and using the linear transformation of the phonon creation and destruction operators (see *Appendix* in Ref. [17]), we can obtain the following expressions for the functions $u_{\lambda\mathbf{q}}$:

$$u_{\lambda\mathbf{q}}(\mathbf{r}) = \left(\frac{2\hbar}{NM\omega_{\mathbf{q}}}\right)^{1/2} \frac{4\pi\gamma e}{q} c_\lambda(\mathbf{qr}), \tag{2}$$

$$\gamma = (4\pi\varepsilon)^{-1/2}(M/a_0^3)^{1/2}\omega_{\mathrm{LO}},$$

$$\varepsilon^{-1} = \varepsilon_\infty^{-1} - \varepsilon_0^{-1},$$

where ε_0 is the static permittivity, ε_∞ is the dielectric constant at a frequency much higher than infrared frequencies (of the order of ω_{LO}) and much lower optical frequencies (of the order of the band gap); N is the number of lattice cells in a crystal; a_0 is the lattice constant; $c_1(\mathbf{qr}) = -\sin(\mathbf{qr})$, $c_2(\mathbf{qr}) = \cos(\mathbf{qr})$.

The Born-Oppenheimer equations can be easily solved in the first order of perturbation theory using the operator H_{eL}. The probability of nonradiative electron transitions between defect levels can be expressed in terms of the matrix elements of this operator on the electron wave functions of the zero approximation $\psi^{(0)}(\mathbf{r})$ [15]. It satisfies the Schrodinger equation with the Hamiltonian, which includes only the interaction energy of the electron with the defect $V_d(\mathbf{r})$:

$$(K + V_d)\psi^{(0)} = W^{(0)}\psi^{(0)}, \tag{3}$$

where K is the kinetic energy operator.

The total energy of an electron-vibrational system corresponding to an electron in a defect state with the wave function $\psi_j^{(0)}$ and with the energy $W_j^{(0)}$ [15]:

$$E_{j\{n\}} = W_j^{(0)} + D_j + \Sigma_{\lambda\mathbf{q}}\hbar\omega_{\mathbf{q}}(n_{\lambda\mathbf{q}} + 1/2), \tag{4}$$

where $\{n\}$ is the set of filling numbers $n_{\lambda\mathbf{q}}$ of phonon modes $(\lambda, \mathbf{q})$, D_j is the deformation energy:

$$D_j = -\frac{1}{2}\Sigma_{\lambda,\mathbf{q}}\hbar\omega_{\mathbf{q}}\left(\eta_{\lambda\mathbf{q}}^{(j)}\right)^2, \tag{5}$$

where $\eta_{\lambda\mathbf{q}}^{(j)}$ is the displacement of the equilibrium position of the lattice oscillator:

$$\eta_{\lambda\mathbf{q}}^{(j)} = -\frac{\langle\psi_j^{(0)}|u_{\lambda\mathbf{q}}|\psi_j^{(0)}\rangle}{\hbar\omega_{\lambda\mathbf{q}}}. \tag{6}$$

For continuum states, the displacement $\eta_{\lambda\mathbf{q}}^{(j)}$ can be set to zero. The wave functions of the electrons of the conduction band were approximated by plane waves, and approximate model wave functions were used for localized vacancy states.

2.2. Model wave functions of a vacancy

The equation of the zero approximation (3) was solved in the Kane model 6×6, the details of the method are described in Ref. [18]. The conduction band, the bands

of light and heavy holes were included in the consideration. When calculating the probability of multiphonon nonradiative transitions, we used a simplified model wave function, the parameters of which were selected taking into account the found Kane wave function. Namely, a two-component wave function was used, in which the first row in the column corresponds to the conduction band, and the second row corresponds to the valence band. The wave function of the state with the wave vector $\mathbf{k}$ in the conduction band:

$$\psi_{\mathbf{k}}(\mathbf{r}) = \begin{pmatrix} V^{-1/2}\exp(\mathbf{kr}) \\ 0 \end{pmatrix}, \tag{7}$$

where V is the main volume of the crystal. The wave function of the state A_2^{-2}:

$$\psi_1(r) = \begin{pmatrix} \alpha\chi_{1s}(a_c, r) \\ \beta\chi_{1s}(a_v, r) \end{pmatrix}, \tag{8}$$

where $\chi_{1s}(a, r)$ is the unit-normalized hydrogen-like wave function of the $1s$-state corresponding to the Bohr radius a ($a = a_c$ for the conduction band and $a = a_v$ for the valence band); α^2 is the proportion of the conduction band in the wave function, $\alpha^2 + \beta^2 = 1$.

The parameters a_c, a_v and α were calculated as follows. The part of the conduction band is a „projection" of the Kane wave function $\psi^{(0)}$ onto the conduction band:

$$\alpha^2 = \langle\psi^{(0)}|J_c|\psi^{(0)}\rangle, \tag{9}$$

where J_c is a matrix 6×6 in which only the diagonal matrix elements in two rows corresponding to the conduction band in the six-component column $\psi^{(0)}$ are nonzero and equal to one; $\langle\psi^{(0)}|\psi^{(0)}\rangle = 1$.

$$a_c = \frac{\langle\psi^{(0)}|rJ_c|\psi^{(0)}\rangle}{\langle\psi^{(0)}|J_c|\psi^{(0)}\rangle}, \tag{10}$$

$$a_v = \frac{\langle\psi^{(0)}|r(I - J_c)|\psi^{(0)}\rangle}{\langle\psi^{(0)}|I - J_c|\psi^{(0)}\rangle}, \tag{11}$$

where I is the identity matrix 6×6.

2.3. Probability of multiphonon transitions and the capture coefficient

We give an expression for the probability of nonradiative transitions [15] in our notation, assuming that the initial state of the electron in the conduction band corresponds to the wave vector $\mathbf{k}$. Assuming the phonon frequency ω independent of the wave vector, we have

$$w(\mathbf{k}) = \Omega_0\Sigma_{m=-2}^{2}\left(\frac{n+1}{n}\right)^{(p-m)/2} g_m(\mathbf{k})I_{p-m}(z), \tag{12}$$

$$\Omega_0 = \omega\,\frac{\pi}{(\hbar\omega)^2}\,e^{-S(2n+1)}, \tag{13}$$

where n is the average number of phonon mode fillings (Bose-Einstein factor), S is the Huang-Rhys factor:

$$S = \Sigma_{\lambda\mathbf{q}}S_{\lambda\mathbf{q}},$$

$$S_{\lambda\mathbf{q}} = \frac{1}{2}\left(\eta_{\lambda\mathbf{q}}^{(\mathbf{k})} - \eta_{\lambda\mathbf{q}}^{(1)}\right)^2 \approx \frac{1}{2}\left(\eta_{\lambda\mathbf{q}}^{(1)}\right)^2, \tag{14}$$

where $\eta_{\lambda\mathbf{q}}^{(1)}$ and $\eta_{\lambda\mathbf{q}}^{(\mathbf{k})}$ are the displacements of the equilibrium centers (6) of lattice oscillators, respectively, for the A_2^{-2} state and the continuum of the conduction band. If the volume is $V \to \infty$, then the offsets $\eta_{\lambda\mathbf{q}}^{(\mathbf{k})}$ are infinitesimal, of a higher order than $\eta_{\lambda\mathbf{q}}^{(1)}$, and they can be ignored. In particular, the deformation energy (5) $D_{\mathbf{k}}$ for the electron state with the wave vector $\mathbf{k}$ in the continuum is zero at $V \to \infty$ ($N \to \infty$), in contrast to the deformation energy for the localized state, which is finite at the specified limiting transition.

Other notation in the formula (12):

$$p = p(\mathbf{k}) = \frac{E_T(\mathbf{k})}{\hbar\omega}, \tag{15}$$

where E_T is the transition energy (energy difference (4) for states involved in the transition at fixed phonon filling numbers):

$$E_T(\mathbf{k}) = W_{\mathbf{k}}^{(0)} - W_1^{(0)} - D_1. \tag{16}$$

Here $W_{\mathbf{k}}^{(0)} = E_c + \hbar^2k^2/(2m_c)$ is the energy of the electron in the conduction band, E_c is the energy of the bottom of the conduction band, m_c is the effective mass of the electron, $W_1^{(0)}$ is the energy of an electron in the A_2^{-2} state of the vacancy, D_1 is the deformation energy corresponding to this state. The energy $W_1^{(0)}$ was calculated in the Kane model taking into account the chemical shift. The chemical shift was calculated using the model potential of the central cell, which was selected in the same way as in Ref. [19], in the form of a shielded point charge potential, with the dielectric constant and the length of the shielding as the fitting parameters. These parameters were selected to achieve a correspondence between the calculated values of the vacancy binding energy and the data on the red boundary of the photoelectric effect obtained from the photocurrent spectra. In the adjustment procedure, the effect of the deformation energy was not taken into account, assuming that $D_1 = 0$. Further,

$$z = 2S\big(n(n+1)\big)^{1/2}, \tag{17}$$

$I_p(z)$ is the modified Bessel function.

The notation for g_m is given taking into account the equalities $\eta_{\lambda\mathbf{q}}^{(\mathbf{k})} = 0$:

$$g_0(\mathbf{k}) = 2^{-1}\big(1 - 2n(n+1)\big)|V_{\mathbf{k}}\eta|^2,$$

$$g_1(\mathbf{k}) = (n+1)(|V_{\mathbf{k}}|^2 - |V_{\mathbf{k}}\eta|^2),$$

$$g_{-1}(\mathbf{k}) = n\big(|V_{\mathbf{k}}|^2 + |V_{\mathbf{k}}\eta|^2\big), \tag{18}$$

$$g_2(\mathbf{k}) = 2^{-1}(n+1)^2|V_\mathbf{k}\eta|^2,$$

$$g_{-2}(\mathbf{k}) = 2^{-1}n^2|V_\mathbf{k}\eta|^2,$$

$$|V_\mathbf{k}|^2 = \Sigma_{\lambda\mathbf{q}}|\langle\psi_1|u_{\lambda\mathbf{q}}|\psi_\mathbf{k}\rangle|^2, \quad (19)$$

$$|V_\mathbf{k}\eta|^2 = |\Sigma_{\lambda\mathbf{q}}\langle\psi_1|u_{\lambda\mathbf{q}}|\psi_\mathbf{k}\rangle\eta^{(1)}_{\lambda\mathbf{q}}|^2, \quad (20)$$

where model wave functions (7) and (8) are used to calculate matrix elements and displacements (6), respectively, for the continuum of the conduction band and A_2^{-2} states. The functions $g_m(\mathbf{k}) = g_m(k)$ in this approximation depend only on the modulus of the vector k.

Let's obtain the capture coefficient c by averaging the probability of transition (12) over the electron distribution function in the zone, assuming the main volume V in the expression (7) for the continuum wave function equal to one:

$$c = \frac{\int w(\mathbf{k})f(\mathbf{k}, T_e)d\mathbf{k}}{\int f(\mathbf{k}, T_e)d\mathbf{k}}. \quad (21)$$

The electron temperature T_e was generally assumed to be different from the crystal temperature T. The distribution function in the calculations was assumed to be Boltzmann, which implies a fairly low concentration of electrons and their non-zero temperature.

3. Results and discussion

3.1. Energy and wave functions

The parameters of MCT semiconductors (parameters of the Kane Hamiltonian, dielectric constant, and band gap), known from the literature, were used for calculations [20,21]. Figure 1 shows the dependence of the binding energy of a single ionized mercury vacancy (A_2^{-1}-center) on the cadmium content in solution. Taking into account the chemical shift, this energy is approximately half as low as without it, and, moreover, it is less dependent on the cadmium content. Calculations in the Kane model of the bond energy and parameters of the model wave function (localization radii and the share of the conduction band in the wave function) were performed at a temperature of 77 K, and their temperature dependence was ignored.

The parameters of the model wave function are shown in Figure 2. Figure 2, *a* shows the localization radii (10) and (11) corresponding to the conduction band and the valence band. It should be noted that they are comparable to each other in magnitude over the entire range of x, despite the significant distance of the conduction band from the vacancy level in comparison with the valence band. Despite the fact that there are contributions to the Kane vacancy wave function with significantly different localization scales, the average characteristic scales determined by the above averaging formulas turn out to be comparable as a result of mixing the components of the wave function with the defect potential. At the same time, strongly localized contributions do not significantly affect the average radii a_c and a_v.

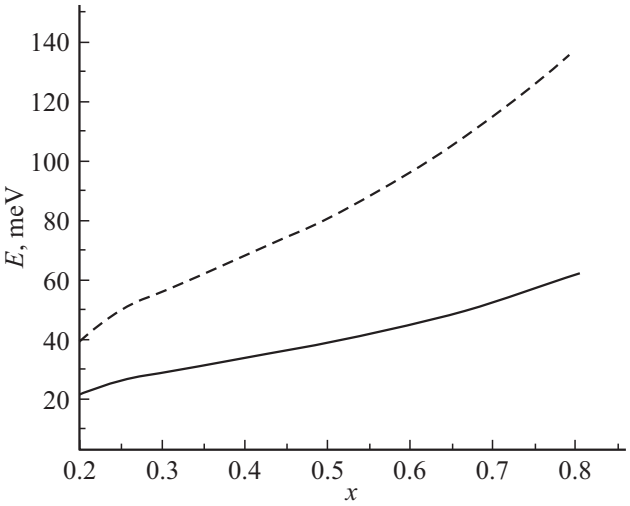

Figure 1. The binding energy of a single ionized mercury vacancy (A_2^{-1}-center) in $Cd_xHg_{1-x}Te$, taking into account the chemical shift (solid line) and without it (dotted line).

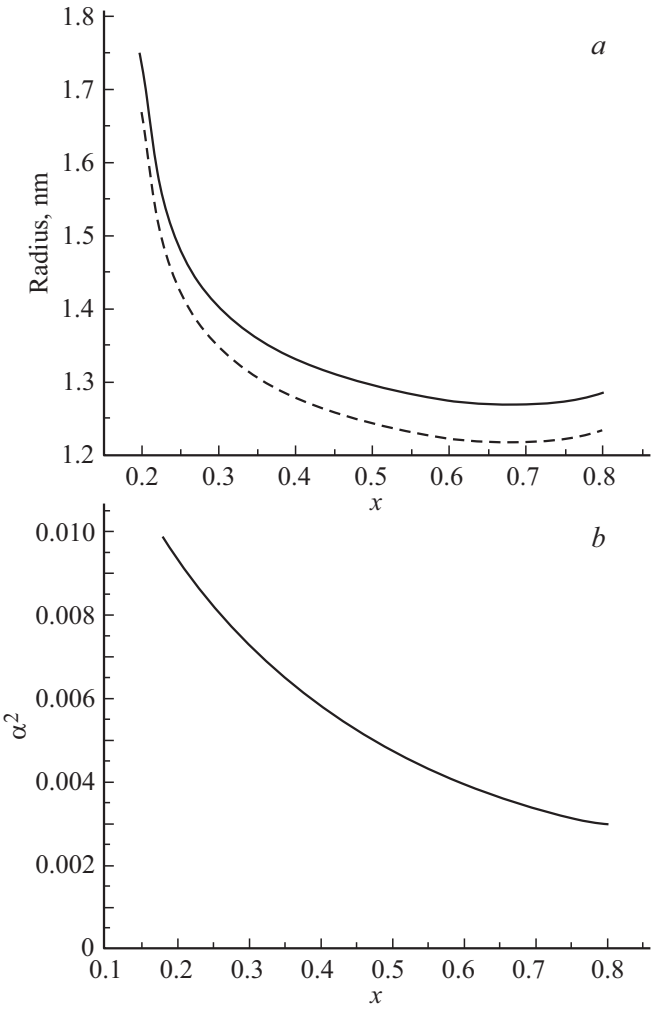

Figure 2. Parameters of the model wave function of a single ionized mercury vacancy (A_2^{-1}-center) in $Cd_xHg_{1-x}Te$: *a* — radii of localization of the wave function for the component corresponding to the valence band (dotted line) and the conduction band (solid line); *b* — the share of the conduction band α^2 in the wave function.

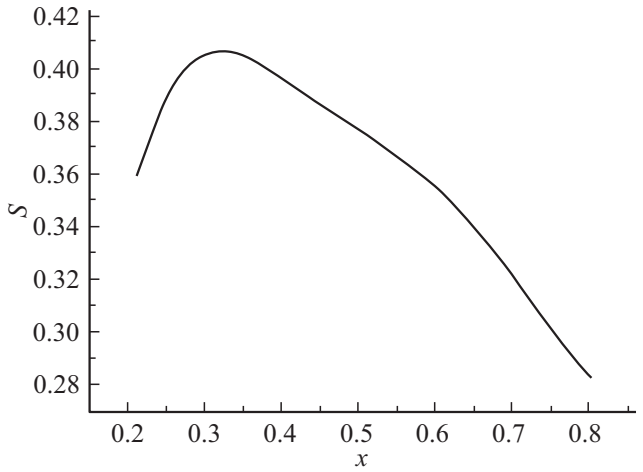

Figure 3. Huang-Rhys factor for the transition of an electron from the conduction band to the ground state of the A_2^{-1}-center in $Cd_xHg_{1-x}Te$.

The share of the conduction band in the wave function as a function of the cadmium content in the solution is shown in Figure 2, *b*. This value can be approximated with a good accuracy by the following expression:

$$\alpha^2 = b + A\exp(-x/x_s), \tag{22}$$

$$b = 1.84 \cdot 10^{-3}, \quad A = 1.42 \cdot 10^{-2}, \quad x_s = 0.315.$$

The Huang-Rhys factor S is shown in Figure 3. The contribution of the conduction band was neglected for calculating it using the model wave function (8), since $\alpha \ll 1$. For any cadmium content, the Huang-Rhys factor is more than 2 times less than unity, which corresponds to a weak electron-phonon coupling. This is primarily due to the rather large radius of localization of the vacancy wave function in comparison with the lattice constant a_0. For reference, we present a simple analytical estimate for S, which is the main term of the asymptotic expansion for $a_0/a_v \ll 1$:

$$S \approx \frac{5\pi\gamma^2 e^2 a_0^3}{16M\hbar\omega^3 a_v}.$$

Calculations in the Kane model, taking into account the chemical shift, give results close to those shown in Figure 3. For example, for $x = 0.21$ $S \approx 0.34$, for $x = 0.25$ $S \approx 0.37$.

3.2. Capture coefficient

The temperature dependence of the capture coefficient on the A_2^{-1} center is shown in Figure 4. First of all, we note that the capture coefficient strongly depends on the cadmium content in the solution: it decreases by several orders of magnitude as x increases from 0.21 to 0.25. This is attributable to an increase in the band gap and transition energy with an increase in the proportion of cadmium. The significant sharpness of the dependence of the capture coefficient on the transition energy is a consequence of the weak electron-phonon coupling ($S \ll 1$). In this case, at low temperatures, a strong additional factor appears that reduces the capture rate with increasing transition energy, since the transition probability is proportional to the ratio $S^p/\Gamma(p)$ [15] ($\Gamma(p)$ is the Gamma function), p is the transition energy expressed in the number of phonon quanta (15). (For reference, the energy of a LO-phonon at room temperature is 20.7 meV in CdTe and 16.7 meV in HgTe [20].) At the same time, the low temperature regime,

$$z \ll p, \tag{23}$$

z is determined by the formula (17), is valid for wide-bandgap MCT up to room temperature.

Next, we note the decreasing nature of the temperature dependence of the capture coefficient, and this dependence is also very sharp. The nature of this dependence is explained by the simultaneous action of two factors. On the one hand, the band gap in the MCT increases quite rapidly with temperature. On the other hand, the weakness of the electron-phonon coupling, due to the proportionality of the probability of multiquantum transitions to the factor $S^p/\Gamma(p)$, leads to a very sharp decrease in the capture coefficient with increasing transition energy with increasing temperature. At the same time, this tendency to inhibit capture cannot be overcome by temperature stimulation of capture, proportional to the factor $(n+1)^p$ [15].

The above arguments and conclusions, which follow from the nature of the dependence of the probability of electron capture on the transition energy, remain valid after averaging this probability over the distribution function (21) when calculating the capture coefficient. Let's make an analytical estimate of the capture coefficient, limiting ourselves

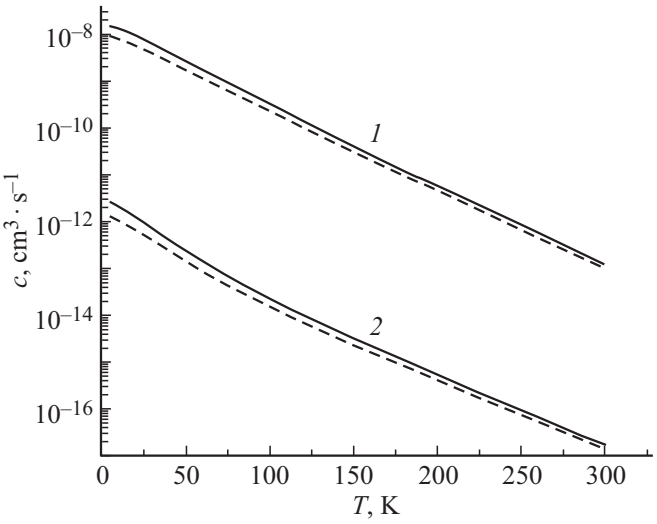

Figure 4. Capture coefficient of conduction band electrons on mercury vacancies (A_2^{-1}-centers) in $Cd_xHg_{1-x}Te$ solution with cadmium content $x = 0.21$ (curves *1*) and $x = 0.25$ (curves *2*). Solid lines show temperature dependences when the electronic temperature T_e coincides with the lattice temperature T, dotted lines show temperature dependences when $T_e = T + 50$ K.

to essentially multi-quantum transitions, $p \gg 1$ ($x > 0.2$). Let's use the asymptotic expansion for large orders, $p \gg z$, for the modified Bessel functions $I_p(z)$ [22]. Let's use the formula (21) to average over the Maxwell distribution function, calculating the integral using the saddle-point method, assuming the inequality $p_0 = E_T(0)/(\hbar\omega) \gg 1$:

$$c \approx \Omega_0 \Sigma^2_{m=-2} (n+1)^{p_m+\gamma_m} w_m, \tag{24}$$

$$w_m = 4\left(\frac{\hbar\omega\gamma_m}{k_B T_e}\right)^{3/2} \varphi_m B_m(z) \exp\left(-\frac{\hbar\omega\gamma_m}{k_B T_e}\right), \tag{25}$$

$$B_m(z) = \frac{S^{p_m+\gamma_m}}{\Gamma(p_m+\gamma_m+1)} \left(1+\left(\frac{z}{p_m}\right)^2\right)^{-1/4} \exp\left(\frac{z^2}{4p_m}\right), \tag{26}$$

$$\gamma_m = \left[2\left(\ln\left(\frac{p_m}{(n+1)S}\right) + \frac{\hbar\omega}{k_B T_e} + \left(\frac{z}{2p_m}\right)^2\right)\right]^{-1}, \tag{27}$$

$$p_m = p_0 - m,$$

$$\varphi_m = (n+1)^{-m} g_m(k_m), \tag{28}$$

$$k_m = \sqrt{2m_c \hbar\omega\gamma_m}\,/\hbar, \tag{29}$$

where m_c is the effective mass in the conduction band. When deriving expressions, the Stirling formula was used for the function $\Gamma(p)$ [22].

The function $B_m(z)$ strongly depends on the index m, which leads to a significant dominance in the sum (24) of the term with $m = 2$ over a wide temperature range. Let's calculate this term by using $k_m \approx 0$ in the formula (28), which is valid for $k_m a_v \ll 1$ and $k_m a_c \ll 1$, and in this case these inequalities are fulfilled. We obtain

$$\varphi_2 = \frac{8\pi^3\alpha^2 a_0^6 a_c (\gamma e)^4 (\lambda^2/4 + 3\lambda/2 + 1)^2}{M^2\omega^4(\lambda/2+1)^6}, \tag{30}$$

where $\lambda = a_v/a_c$. The inequality $\alpha \ll 1$ was used for calculating φ_2. Then the capture coefficient is

$$c \approx \Omega_0 (n+1)^{p_2+\gamma_2} w_2, \tag{31}$$

where all the values in this formula are determined by the formulas (13), (25)–(27), (30). $p_2 + \gamma_2 \approx p_2$ can be used in these formulas at the cost of a slight deterioration in accuracy.

The strongest dependence on the transition energy is given by the multiplier $B_m(z)$ (26), which is proportional to the ratio $S^{p_0}/\Gamma(p_0)$, $p_0 = E_T(0)/(\hbar\omega)$. For weak and moderately weak electron-phonon coupling ($S < 1$), the numerator and denominator of this ratio affect capture in the same way: both impose a decreasing dependence of the capture coefficient on p_0, and this dependence is especially sharp with a strong inequality $S \ll 1$. This explains the strong dependence of the electron capture rate on the cadmium content x and temperature T.

Let's compare the capture coefficient with the recently obtained calculation results in the semiclassical approximation [11], limiting ourselves to the case of „wide-bandgap" MCT ($x > 0.2$). Firstly, for a fixed temperature, the calculations in this paper give a much more significant dependence of the capture coefficient on the cadmium content compared to the semiclassical method. For example, according to Ref. [11], at a temperature of $T = 100$ K, an increase in the cadmium content x from 0.22 to 0.24 leads to a decrease in the capture coefficient from $\sim 8 \cdot 10^{-9}$ cm$^3 \cdot$ s^{-1} to $\sim 10^{-9}$ cm$^3 \cdot$ s^{-1}. On the contrary, calculations in this paper at the same temperature at the ends of the similar range x from 0.21 to 0.25 give the capture coefficient of $\sim 3 \cdot 10^{-10}$ cm$^3 \cdot$ s^{-1} and $\sim 2 \cdot 10^{-14}$ cm$^3 \cdot$ s^{-1} respectively. Namely, the value of the capture coefficient turns out to be significantly lower, and the effect of the composition of the MCT solution on electron capture is much more significant.

Secondly, the present paper gives a much more significant temperature dependence of the capture coefficient (the change of several orders of magnitude in the temperature range from 60 to 100 K) compared with the calculations in Ref. [11] (the change is no more than a few tens of percent in the same temperature range, and it is not more than 3 fold at $x < 0.2$).

The reason for such significant discrepancies is that the semiclassical calculations [11] used formulas (see Ref. [23]) for the thermal activation regime in the temperature range beyond its applicability. The quantum approach [15] provides an accurate criterion for the thermal activation regime:

$$2S[n(n+1)]^{1/2} \gg p. \tag{32}$$

The opposite criterion (23) of low temperatures holds for wide-bandgap MCT semiconductors up to room temperature. It is at low temperatures that an extremely strong dependence of the capture rate on the transition energy occurs, which, in approximate estimates, is described by a multiplier B_m (26) proportional to S^{p_0} and inversely proportional to the Gamma function $\Gamma(p_0)$.

It should be noted that with a decrease in the cadmium content, the inequality (23) weakens or is violated, therefore, the discrepancy between the results of this study and the study in Ref. [11] is significantly reduced. In case of a decrease in the cadmium content to $x = 0.177$, when the capture of electrons from the conduction band becomes possible by emitting single optical phonons, semiclassical estimates of the capture coefficient [11] are in good agreement with rigorous quantum mechanical calculations for single-quantum capture processes [10].

With this in mind, based on the analysis of experimental data on the temporal dynamics of the photocurrent [11], it is possible to conclude that electron capture on mercury vacancies as part of the Shockley-Read-Hall recombination mechanism may play a significant role in electron recombination in a certain narrow range of compositions with cadmium content at $x < 0.2$ near $x = 0.2$. In this case, the recombination of SRH through mercury vacancies can play a significant role for low electron concentrations, competing with Auger recombination. On the contrary, in wide-bandgap MCT ($x > 0.2$) the recombination of SRH

through mercury vacancies is strongly suppressed, so it occurs through deeper traps.

4. Conclusion

The capture coefficient of conduction-band electrons on mercury vacancies (acceptor A_2^{-1}-centers) in „wide-band“ ($x > 0.2$) $Cd_xHg_{1-x}Te$ semiconductors is estimated using the adiabatic approximation. It is shown that the capture coefficient sharply decreases with an increase in the cadmium content x. For example, the low-temperature capture coefficient decreases from $\sim 10^{-8}\,cm^3 \cdot s^{-1}$ at $x = 0.21$ to $\sim 10^{-12}\,cm^3 \cdot s^{-1}$ for $x = 0.25$. The significant suppression of multiphonon capture with an increase in the cadmium content is explained by an increase in the transition energy combined with the weakness of electron-phonon coupling for electrons localized in vacancies (Huang-Rhys factor $S < 0.5$), and a significant distance of vacancy levels from the bottom of the conduction band. The weakness of the electron-phonon coupling is mainly attributable to the relatively large radius of electron localization in the vacancy. This leads to a strong localization of the vacancy wave functions in the momentum space (typical for defects with shallow levels), which limits the number of bulk phonon modes with which electrons effectively interact in multiquantum processes.

Deeper defects than mercury vacancies play a significant role in the interband nonradiative electron recombination in wide-bandgap CdHgTe layers.

Funding

Calculations of the hole energies at the acceptor centers, the localization scales of their wave functions, and the fractions of the conduction band in these functions were performed within the framework of the IAP RAS state assignment, project FFUF-2024-0019. Calculations of electron capture coefficients for acceptor centers were carried out with the support of the Russian Science Foundation (grant No. 22-12-00298).

Conflict of interest

The authors declare that they have no conflict of interest.

References

[1] M. Orlita, K. Masztalerz, C. Faugeras, M. Potemski, E.G. Novik, C. Brüne, H. Buhmann, L.W. Molenkamp. Phys. Rev. B, **83**, 115307 (2011).
[2] B.A. Bernevig, T.L. Hughes, S.-C. Zhang. Science, **314**, 1757 (2006).
[3] M. König, S. Wiedmann, C. Brüne, A. Roth, H. Buhmann, L.W. Molenkamp, X.-L. Qi, S.-C. Zhang. Science, **318**, 766 (2007).
[4] M. Orlita, D.M. Basko, M.S. Zholudev, F. Teppe, W. Knap, V.I. Gavrilenko, N.N. Mikhailov, S.A. Dvoretskii, P. Neugebauer, C. Faugeras, A.-L. Barra, G. Martinez, M. Potemski. Nature Physics, **10**, 233 (2014).
[5] A. Rogalski. Opto-Electron. Rev., **20**, 279 (2012).
[6] S.V. Morozov, V.V. Rumyantsev, M.A. Fadeev, M.S. Zholudev, K.E. Kudryavtsev, A.V. Antonov, A.M. Kadykov, A.A. Dubinov, N.N. Mikhailov, S.A. Dvoretsky, V.I. Gavrilenko. Appl. Phys. Lett., **111**, 192101 (2017).
[7] K.E. Kudryavtsev, V.V. Rumyantsev, V.V. Utochkin, M.A. Fadeev, V.Ya. Aleshkin, A.A. Dubinov, M.S. Zholudev, N.N. Mikhailov, S.A. Dvoretskii, V.G. Remesnik, F. Teppe, V.I. Gavrilenko, S.V. Morozov. J. Appl. Phys., **130**, 214302 (2021).
[8] W. Shockley, W.T. Read, jr. Phys. Rev., **87**, 835 (1952).
[9] R.N. Hall. Phys. Rev., **87**, 387 (1952).
[10] D.V. Kozlov, V.V. Rumyantsev, A.A. Yantser, S.V. Morozov, V.I. Gavrilenko. JETP **165** (6), 852 (2024).
[11] D.V. Kozlov, A.V. Ikonnikov, K.A. Mazhukina, S.V. Morozov, V.I. Gavrilenko, N.N. Mikhailov, S.A. Dvoretsky, V.V. Rumyantsev. Semicond. Sci. Technol., **40**, 035007 (2025).
[12] V.A. Kovarskii, N.F. Perel'man, I.Sh. Averbukh. *Mnogokvantovye protsessy* (M., Energoatomizdat, 1985). (in Russian).
[13] D.V. Kozlov, V.V. Rumyantsev, S.V. Morozov, A.M. Kadykov, M.A. Fadeev, H.-W. Hübers, V.I. Gavrilenko. Semiconductors, **52**, 1369 (2018).
[14] I.B. Bersuker. *The Jahn-Teller Effect* (Cambridge University Press, UK, 2006).
[15] E. Gutsche. Phys. Status Solidi B, **109**, 583 (1982).
[16] V.F. Gantmakher, I.B. Levinson. *Rasseyanie nositelej toka v metallakh i poluprovodnikakh* (M., Nauka, 1984). (in Russian).
[17] N.A. Bekin, R.Kh. Zhukavin, V.V. Tsyplenkov, V.N. Shastin. Semiconductors, **58**, 7 (2024).
[18] D.V. Kozlov, V.V. Rumyantsev, S.V. Morozov, A.M. Kadykov, M.A. Fadeev, H.-W. Hübers, V.I. Gavrilenko. Semiconductors, **52**, 1369 (2018).
[19] N.O. Lipari, A. Baldereschi, M.L.W. Thewalt. Solid State Commun., **33**, 277 (1980).
[20] S. Adachi. *Properties of Group-IV, III–V and II–VI Semiconductors* (John Wiley & Sons, Ltd, 2005).
[21] J.P. Laurenti, J. Camassel, A. Bouhemadou, B. Toulouse, R. Legros, A. Lusson. J. Appl. Phys., **67**, 6454 (1990).
[22] *Handbook of Mathematical Functions With Formulas, Graphs, and Mathematical Tables*, ed. by M. Abramowitz, I. Stegun. National Bureau of Standards Applied Mathematics Series 55, 1972.
[23] V.N. Abakumov, V.I. Perel', I.N. YAssievich. *Bezyzluchatel'naya rekombinaciya v poluprovodnikah* (SPb., Izd-vo „Peterburgskij institut yadernoj fiziki im. B.P. Konstantinova RAN“, 1997). (in Russian).

Translated by A.Akhtyamov